

# Influence of the martensitic transformation on the deformation behaviour of an AISI 316 stainless steel at low temperatures

V. SEETHARAMAN

Reactor Research Centre, Kalpakkam 603102, India

R. KRISHNAN

Bhabha Atomic Research Centre, Bombay 400085, India

The deformation behaviour of an AISI 316 stainless steel under uniaxial tension was examined at 25, -70 and -196°C. The flow curves exhibited peculiar shapes and the work hardening rates were found to increase with strain beyond certain values of plastic strain. X-ray diffraction analyses showed that the transformation to  $\alpha$ -martensite commenced at these values of plastic strain and thereafter the volume fraction of  $\alpha$  increased steadily with strain. On the other hand, the amount of the  $\epsilon$ -martensite was found to increase with plastic strain initially, reach a maximum and then decrease gradually. The contribution of the  $\alpha$ -phase to the flow stress of the alloy was found to be directly proportional to the volume fraction of  $\alpha$ . It is shown that the analysis of the flow curves provides a simple method of detecting the onset of the strain-induced martensitic transformation as well as estimating the amount of this martensite during further deformation.

## 1. Introduction

It is well known that plastic deformation at low temperatures induces martensitic transformation in many austenitic stainless steels [1-3]. However, it has been recognized only relatively recently that such a strain-induced transformation of austenite is responsible for significant changes in mechanical properties like flow stress, work hardening rates, fracture toughness and low cycle fatigue characteristics of these steels [4-6]. Guimaraes and De Angelis [7, 8] have put forth theoretical models to explain these effects and have used them to substantiate the unique combination of mechanical properties exhibited by many TRIP steels.

Manganon and Thomas [9] have investigated the tensile properties of a type 304 stainless steel containing  $\alpha$ -martensite produced by deformation at sub-zero temperatures both with and without subsequent ageing in the range 150 to 400°C. They have concluded that the yield strength of the steel is proportional to the volume fraction of the  $\alpha$ -martensite, irrespective of the specific

thermomechanical treatment employed to obtain this amount of  $\alpha$ -phase. Rosen *et al.* [4] have found that the fracture strain obtained in tensile tests reaches a maximum at a temperature between  $M_s$  and  $M_d$  (the maximum temperatures at which the transformation to martensite occurs spontaneously and under mechanical activation are denoted as  $M_s$  and  $M_d$  respectively). This temperature remains unaffected by changes in the strain rate and the austenite grain size. Bhandarkar *et al.* [6] have studied the relationship between the stability of the austenite and its tensile properties in a series of Fe-Ni-Cr-C alloys and have demonstrated that it is possible to produce metastable austenitic steels having a wide range of mechanical properties.

The co-existence of the  $\gamma$ -,  $\epsilon$ -, and  $\alpha$ -phases in most of the deformed stainless steels has led to a controversy regarding the sequence in which these phases form. Although the bulk of the experimental data seem to favour the sequence  $\gamma \rightarrow \epsilon \rightarrow \alpha$ , it must be admitted that this controversy has not been resolved satisfactorily.

TABLE I Chemical composition of the AISI 316 stainless steel (wt%)

C	Cr	Ni	Mo	Si	Mn	S	P	Fe
0.05	17.45	11.81	2.5	0.68	1.35	0.011	0.047	balance

In this paper the deformation characteristics of the austenite in AISI 316 stainless steel are examined at low temperatures. In addition, the X-ray diffraction data regarding the volume fractions of the  $\epsilon$ - and the  $\alpha$ -martensites formed during the course of the tensile deformation of this alloy are reported. Finally, an attempt is made to correlate the flow stress of the alloy with the amount of martensite formed.

## 2. Experimental procedure

The chemical composition of the AISI 316 stainless steel used in this investigation is given in Table I. This alloy was cold rolled into strips of about 0.8 mm thickness and tensile samples with gauge dimensions of 25 mm  $\times$  6.3 mm  $\times$  0.8 mm were machined from these strips. All the samples were encapsulated in evacuated quartz tubes, solution treated at 1050°C for 15 min and quenched in water. After this treatment the alloy was found to contain austenite only and the mean grain size of this austenite, determined by the linear intercept method, was approximately equal to 100  $\mu$ m.

Tensile tests were carried out in an Instron machine at a nominal strain rate of  $6.67 \times 10^{-5} \text{ sec}^{-1}$  at 25,  $-70$  and  $-196^\circ\text{C}$ . Values of true stress, true plastic strain and work hardening rates were obtained by computer analysis of the load-extension curves. The work hardening rates were analysed by the method of Crussard and Jaoul [10]. This analysis assumes that the flow stress,  $\sigma$ , can be related to the true plastic strain,  $\epsilon_p$ , by the expression

$$\sigma = \sigma_0 + h\epsilon_p^m, \quad (1)$$

where  $\sigma_0$ ,  $h$  and  $m$  are constants which can be determined from plots of  $\log(d\sigma/d\epsilon_p)$  against  $\log \epsilon_p$ .

The volume fractions of the  $\alpha$  and  $\epsilon$ -martensites present in the samples deformed to various levels were determined by X-ray diffraction [11] using monochromated  $\text{CrK}\alpha$  radiation. Additionally, a few solution-treated sheets were rolled at  $-196^\circ\text{C}$  to different thicknesses. Samples from these sheets subjected to different amounts of cold reduction were also examined by X-ray diffraction.

## 3. Results and discussion

### 3.1. Tensile deformation behaviour

True stress,  $\sigma$ , against true plastic strain,  $\epsilon_p$ , plots for the solution-annealed samples at various test temperatures are shown in Fig. 1. It can be seen that the room-temperature flow curve becomes almost linear beyond a plastic strain of about 0.05. The other two flow curves corresponding to  $-70$  and  $-196^\circ\text{C}$ , respectively, exhibit slightly different behaviour in that the work hardening rate,  $d\sigma/d\epsilon_p$ , appears to increase with strain beyond a certain value of strain (Fig. 2). Multiple stage work hardening was observed at all test temperatures. While three distinct stages were noticed at  $-196$  and  $-70^\circ\text{C}$ , only two different stages were observed at room temperature. Analysis of the results based on the method suggested by Crussard and Jaoul [10] yielded the values of  $\sigma_0$ ,  $h$  and  $m$  in the different stages as shown in Table II. It appears that at all temperatures, the work hardening rate decreased with plastic strain up to a common value ( $\sim 0.1$ ) of the latter. Thereafter,  $d\sigma/d\epsilon_p$  either increased with  $\epsilon_p$  or remained steady. The rate of change of work hardening rate,  $d \log(d\sigma/d\epsilon_p)/d \log \epsilon_p$ , was found to increase with decreasing test temperature.

The peculiar behaviour of the flow curves particularly at low temperatures, could be attributed to the occurrence of the austenite-martensite transformation during plastic deformation. Fig. 3 demonstrates that the data corresponding to  $-196^\circ\text{C}$  could be approximated by a straight line up to a plastic strain of about 0.1. Thereafter it deviates increasingly from the extrapolated straight line which represents the hypothetical flow curve for the austenite at strains beyond 0.1, in the absence of the martensitic transformation. The difference in stress between the experimental curve and the extrapolated line at any value of plastic strain could be considered as the contribution of the martensite formed to the flow stress of the stainless steel at that value of strain.

It can be seen that the tendency of these curves to exhibit a linear segment decreases rapidly with an increase in test temperature. The room-temperature curve does not contain any linear segment

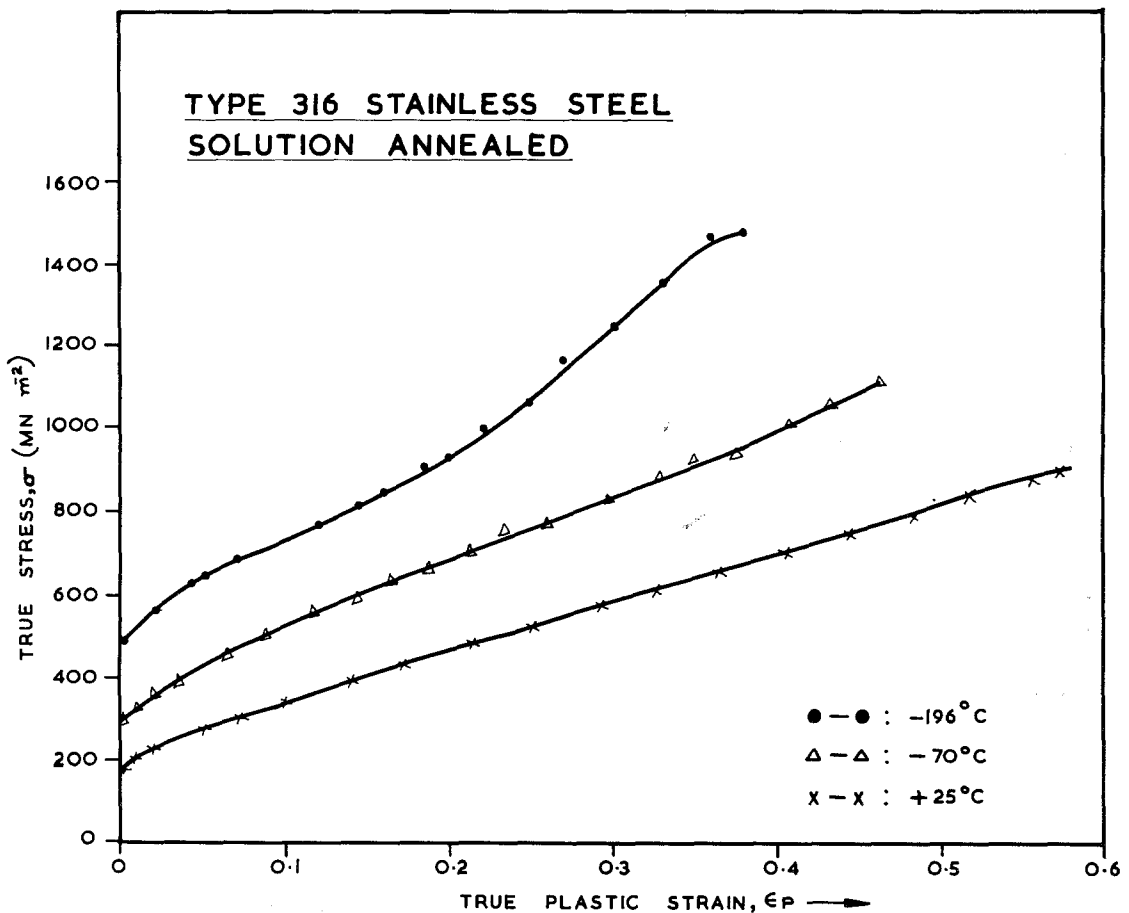


Figure 1 True stress against true plastic strain plots for an AISI 316 stainless steel at low temperatures.

at all. It may be argued that if no martensite formed during deformation at room temperature then the  $\log \sigma \log \epsilon$  curve should be a straight line. However, Ludwigson [12] has shown that the corresponding curves for even the most stable austenites, like those found in type 310 stainless steels, do exhibit considerable deviations from linearity at low values of strain. In fact, he has shown that the flow stress in stable stainless steels is given by a modified form of the Ludwick equation

$$\sigma = K_1 \epsilon^{n_1} + K_2 \exp n_2 \epsilon, \quad (2)$$

where  $K_1$ ,  $K_2$ ,  $n_1$  and  $n_2$  are constants.

### 3.2. X-ray diffraction studies

Analysis of the X-ray data showed that, in general, the deformed samples contained a mixture of three phases: (i) the face centred cubic austenite  $\gamma$ -phase (ii) the hexagonal close packed  $\epsilon$ -phase and (iii) the body centred cubic  $\alpha$ -phase. It should be mentioned that, in this situation, no martensite

formed spontaneously in this alloy on cooling down to  $-196^\circ\text{C}$ . Moreover, it was noticed that the amount of the  $\alpha$ -martensite formed on deformation at 25 or  $-70^\circ\text{C}$  was very small even at very large values of strain. In view of the large errors associated with the quantitative analysis by X-ray diffraction of this phase at very low volume fractions our discussion will be confined only to the martensites produced by deformation at the liquid nitrogen temperature. The observed volume fractions of the  $\epsilon$ - and  $\alpha$ -martensites are shown in Fig. 4 as a function of plastic strain at  $-196^\circ\text{C}$ . The results are compared with those obtained by Manganon and Thomas [13] for a type 304 stainless steel.

The main inferences that can be drawn from Fig. 4 are (i) with increasing plastic strain the amount of the  $\epsilon$ -martensite initially increased until it reached a maximum; thereafter it decreased gradually, (ii) detectable amounts of the  $\alpha$ -phase were formed only beyond a certain minimum

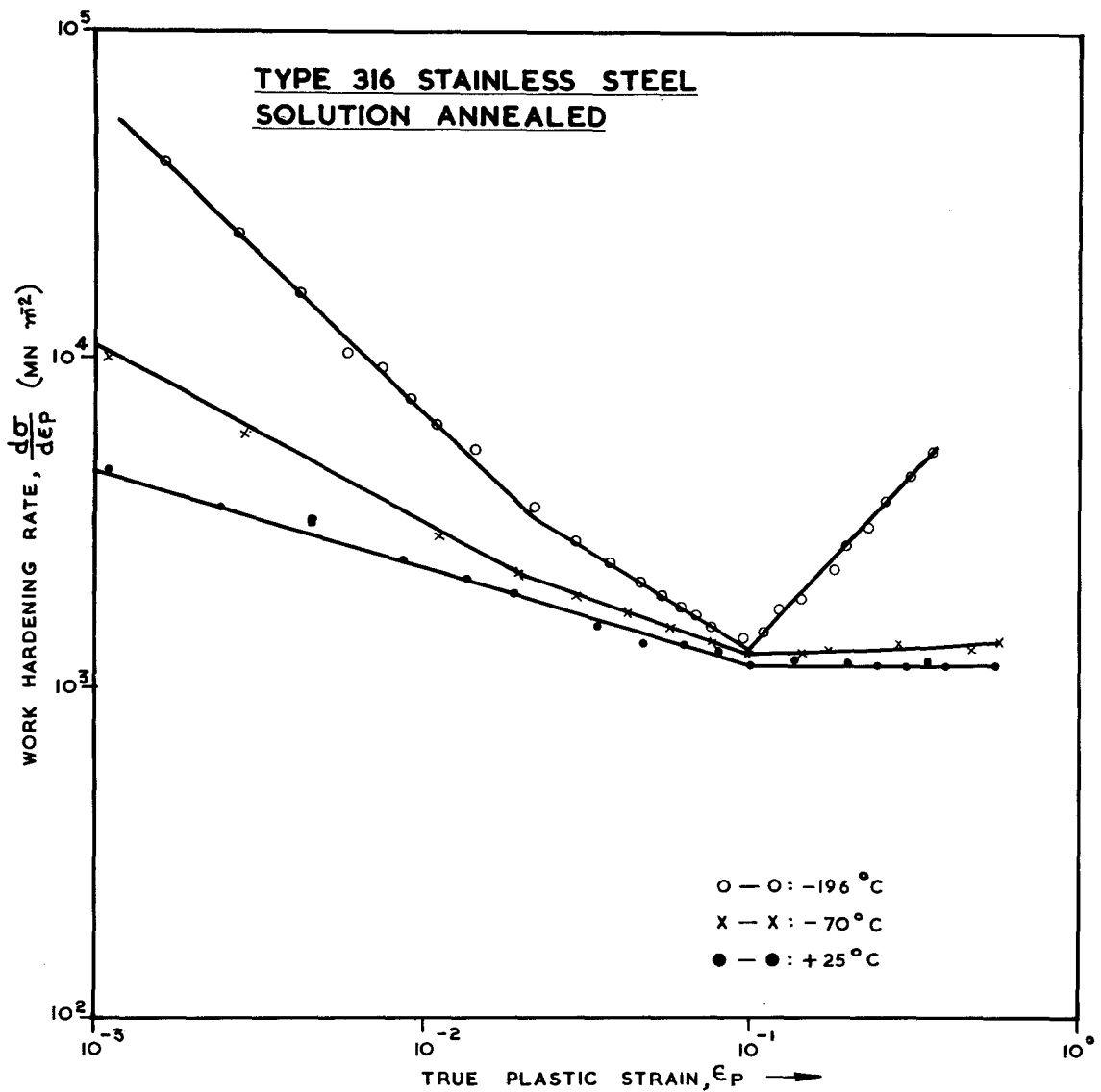


Figure 2 Work hardening rate plotted as a function of plastic strain and test temperature.

TABLE II Work hardening parameters of the AISI 316 stainless steel in the solution treated condition

$T$ (°C)	Stage	$\sigma_0$ (MN m <sup>-2</sup> )	$h$ (MN m <sup>-2</sup> )	$m$
-196	I	520	1500	0.06
	II	384	842	0.389
	III	906	6810	2.47
-70	I	170	770	0.35
	II	80	1225	0.45
	III	210	1430	1.05
25	I	43	1335	0.45
	II	220	1200	1.0

value of plastic strain (0.1 to 0.15); thereafter, the volume fraction of  $\alpha$ -phase increased continuously with plastic strain, (iii) at any particular value of the true plastic strain, the amount of the  $\alpha$ -phase formed in samples deformed by rolling is larger than that in samples deformed in tension, probably due to the higher strain rates and the operation of a biaxial stress system in the former mode of deformation.

While these results are in qualitative agreement with those reported by other investigators a few differences are worth noting. For instance, the strain

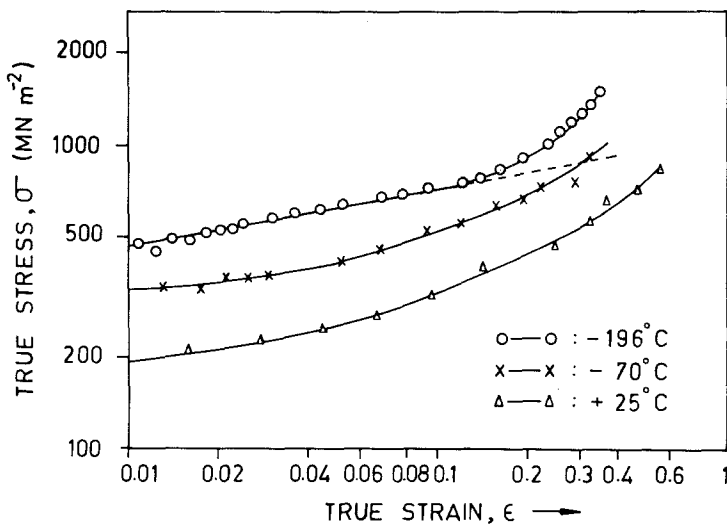


Figure 3 Log  $\sigma$  against log  $\epsilon$  plots showing the deviation from linear behaviour at very low temperatures beyond a certain value of plastic strain.

corresponding to the maximum amount of  $\epsilon$ -phase in AISI 316 stainless steel used in this work was about 0.13 while this figure was reported as 0.05 for a type 304 stainless steel. Again the rate of change of the volume fraction of  $\alpha$ -phase with plastic strain,  $dV_{\alpha}/d\epsilon_p$ , was considerably lower than those values encountered in 18 wt% Cr–8 wt% Ni stainless steels.

vacuum-melted high-purity experimental steel containing 16% Cr, 12% Ni, 0.003% C and 0.009% N, about 85%  $\alpha$  forms after rolling at  $-78^{\circ}\text{C}$  and about 15%  $\alpha$ -phase forms after rolling at  $20^{\circ}\text{C}$ . These results show that the commercial stainless steels are much more resistant to the transformation to martensite than the pure experimental steels.

Coleman and West [14] have reported that in a

It has been established that the martensite

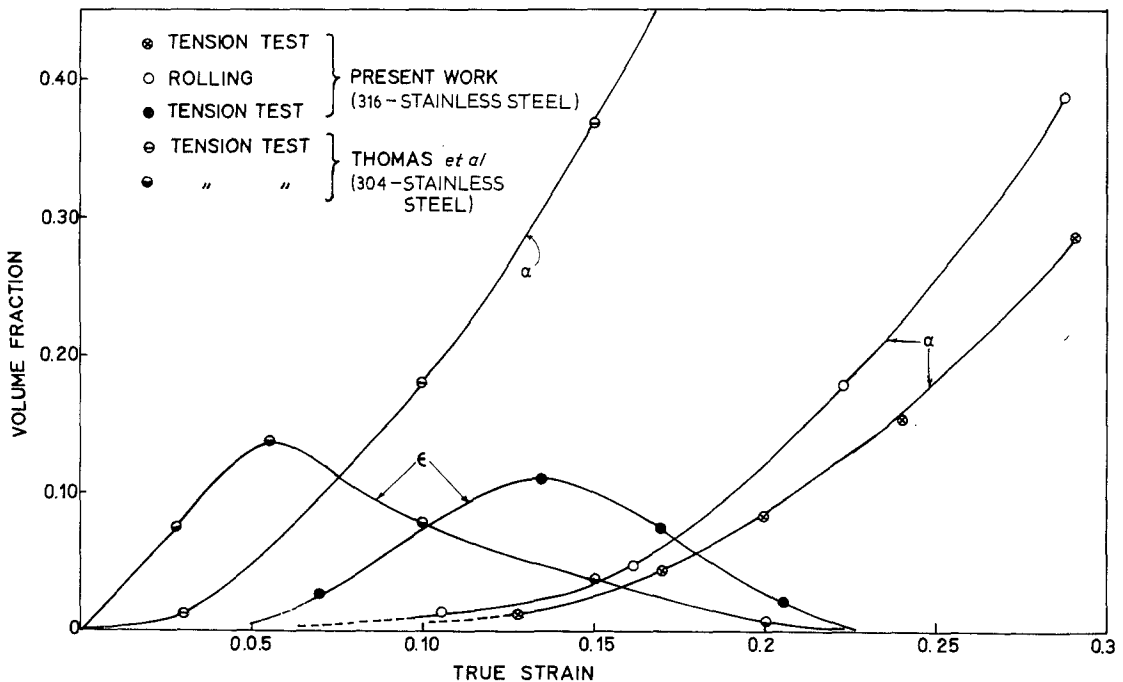


Figure 4 Volume fractions of the  $\epsilon$ - and  $\alpha$ -martensite obtained by X-ray diffraction analysis of samples deformed at  $-196^{\circ}\text{C}$  both in uniaxial tension and by rolling. The corresponding data obtained by Manganon and Thomas [13] in a type 304 stainless steel are also shown for the sake of comparison. Since the  $\alpha$ -phase is ferromagnetic Manganon and Thomas [13] have estimated the volume fraction of  $\alpha$ -phase by measuring the intrinsic saturation magnetization values of the deformed samples. However, they have estimated the  $\epsilon$ -phase by X-ray diffraction.

nucleates at the intersections of two sets of deformation bands formed on  $\{111\}$  planes of the austenite [15, 16]. Since the generation of these deformation bands is closely related to the stacking fault energy,  $\gamma$ , of the austenite, it is clear that this parameter determines the rate of transformation during plastic straining. Based on a multi-dimensional regression analysis Shramm and Reed [17] have established a relationship between the stacking fault energy of the austenite and its chemical composition

$$\begin{aligned} \gamma = & -53 + 6.2 \text{ wt\% Mn} + 0.7 \text{ wt\% Cr} \\ & + 3.2 \text{ wt\% Mn} + 9.3 \text{ wt\% Mo} \text{ mJ m}^{-2}. \end{aligned} \quad (3)$$

Accordingly, the value of  $\gamma$  for the steel used in this work was about  $60 \text{ mJ m}^{-2}$ , while the corresponding values for the austenites encountered in the works of Manganon and Thomas [13] and Coleman and West [14] are 18 and  $50 \text{ mJ m}^{-2}$  respectively. Thus it is clear that the observed differences in the transformation behaviour of these steels can, at least partially, be attributed to the high stacking fault energy of the AISI 316 stainless steel.

The rate at which the volume fraction of the strain-induced martensite,  $V_\alpha$ , changes with plastic strain,  $\epsilon_p$ , can be expressed by the equation [18]

$$V_\alpha = 1 - \exp \{ \beta [1 - \exp(-\alpha \epsilon_p)]^n \}, \quad (4)$$

where  $n$  is a fixed exponent, and  $\alpha$  denotes the rate of shear band formation with respect to plastic strain and is principally dependent on the stacking fault energy of the austenite. The parameter  $\beta$  is linearly related to the probability that a shear band intersection would generate a martensitic embryo and is governed by the chemical driving force for the transformation  $\epsilon \rightarrow \alpha$ . Using the data presented in Fig. 4,  $\alpha$  and  $\beta$  were evaluated for this stainless steel at  $-196^\circ \text{C}$  ( $n$  was assumed to be equal to 4.5 as suggested by Olson and Cohen [18]) as 4.8 and 1.6 respectively. This value of  $\alpha$  was much smaller than that reported by Olson and Cohen [18] for a type 304 stainless steel. This difference could also be attributed to the high stacking fault energy of the austenite in the AISI 316 stainless steel used in this work.

### 3.3. Correlation of the deformation behaviour and the volume fraction of martensite

Examination of the flow curves suggests that the formation of the  $\epsilon$ -phase does not strengthen the austenite to any considerable extent. This is found to be consistent with the observation made by Llewellyn and Murray [19]. However, it can be noticed (Fig. 2) that the first break in the  $\log(d\sigma/d\epsilon_p)$  against  $\log \epsilon_p$  plots corresponding to test temperatures of  $-196$  and  $-70^\circ \text{C}$  occurred at those values of plastic strain at which detectable amounts of the  $\epsilon$ -phase formed. On the other hand, there was no corresponding discontinuous change in the work hardening rate at room temperature at strains below 0.1. At the same time, X-ray diffraction results showed that  $\epsilon$ -phase did not form to any significant extent at room temperature. These observations suggest that the formation of the  $\epsilon$ -phase caused the work hardening rates of the steel to remain higher than they would have done had the  $\epsilon$ -phase not formed at all.

Next, the contribution of the  $\alpha$ -martensite formed during deformation to the flow stress of the steel will be considered. This can be obtained by relating the difference in stresses,  $(\sigma - \sigma_\gamma)$ , between the experimental curve and the extrapolated line (Fig. 3) to the volume fraction of the  $\alpha$ -martensite,  $V_\alpha$ , formed at the corresponding strain values. Fig. 5 which shows such a plot of plastic deformation in uniaxial tension at  $-196^\circ \text{C}$  yields the following relation

$$(\sigma - \sigma_\gamma) = 1040 V_\alpha \text{ MN m}^{-2}. \quad (5)$$

This equation suggests that strengthening due to the formation of  $\alpha$ -martensite is similar to that achieved in composite materials (i.e. it obeys the rule of mixtures). The value of the slope,  $\sigma_\alpha = 1040 \text{ MN m}^{-2}$  presumably corresponds to the strength of the fully transformed alloy at  $-196^\circ \text{C}$ . However, this prediction could not be verified in this alloy since the maximum value of  $V_\alpha$  obtained at the end of the uniform elongation was only 0.32. Since  $(\sigma - \sigma_\gamma) = 0$  at  $V_\alpha = 0$ , this method provides a simple technique for identifying the plastic strain at which the  $\alpha$ -martensite begins to form. In other words, this strain could be identified as the point at which the work hardening rate,  $d\sigma/d\epsilon_p$ , begins to increase with plastic strain.

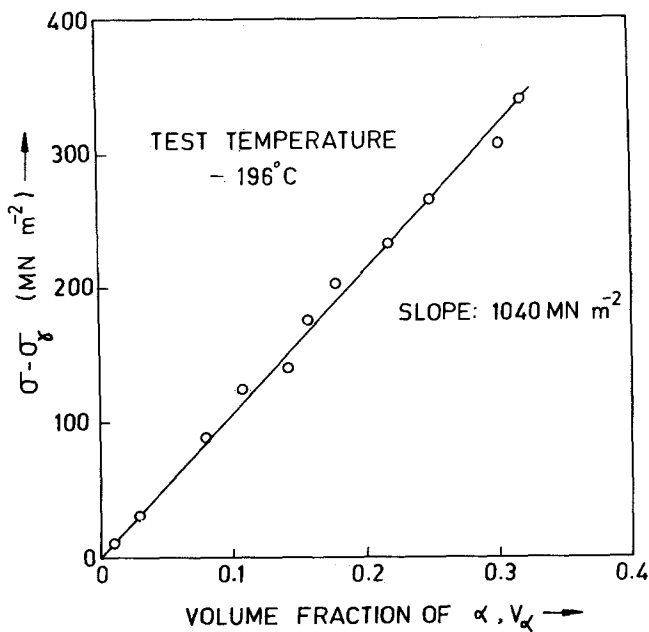


Figure 5 A plot of stress increment,  $\Delta\sigma$  due to the formation of martensite against the volume fraction of the  $\alpha$ -martensite formed at corresponding values of plastic strain.

#### 4. Conclusions

(1) The shape of the true stress–true strain curves is strongly influenced by the test temperature; the formation of strain-induced martensite leads to a peculiar shape of the flow curve.

(2) The work hardening rate decreased with plastic strain up to a certain value of strain, beyond which it increased steeply; this value of strain corresponded to the onset of the transformation to  $\alpha$ -martensite.

(3) The volume fraction of the  $\epsilon$ -martensite initially increased, reached a maximum and thereafter decreased gradually with increasing plastic strain. On the other hand, the amount of  $\alpha$ -phase increases monotonically with plastic strain. Thus the sequence of the transformations in this steel appears to be  $\gamma \rightarrow \epsilon \rightarrow \alpha$ .

(4) The increase in flow stress after the onset of the  $\epsilon \rightarrow \alpha$  transformation is directly proportional to the volume fraction of the martensite present at any particular value of plastic strain.

(5) Analysis of the tensile deformation behaviour provides a simple technique for not only identifying the onset of the strain-induced martensitic transformation but also determining the extent of transformation during subsequent deformation.

#### Acknowledgements

The authors are grateful to Dr M. K. Asundi and Mr C. V. Sundaram, Bhabha Atomic Research

Centre, Bombay, for their encouragement and keen interest in this work. They wish to thank Drs S. Banerjee and P. Mukhopadhyay of BARC, and Drs P. Rodriguez, V. S. Raghunathan and Mr S. Varadaraj of the Reactor Research Centre, Kalpakkam for many valuable suggestions.

#### References

1. J. R. PATEL and M. COHEN, *Acta Met.* 1 (1953) 539.
2. P. M. KELLY and J. NUTTING, *J. Iron Steel Inst.* 197 (1961) 199.
3. T. ANGEL, *ibid.* 177 (1954) 165.
4. A. ROSEN, R. JAGO and T. KJER, *J. Mater. Sci.* 7 (1972) 870.
5. V. F. ZACKAY, E. R. PARKER, D. FAHR and R. BUSCH, *Trans. ASM* 60 (1967) 252.
6. D. BHANDARKAR, V. F. ZACKAY and E. R. PARKER, *Met. Trans.* 3 (1972) 2619.
7. J. R. C. GUIMARAES and R. J. DE ANGELIS, *Mater. Sci. Eng.* 13 (1974) 109.
8. *Idem*, *Met. Trans.* 4 (1973) 2381.
9. P. MANGANON Jr and G. THOMAS, *ibid.* 1 (1970) 1587.
10. C. CRUSSARD and B. JAOUL, *Rev. Met.* 57 (1950) 589.
11. B. D. CULLITY, "Elements of X-ray Diffraction" (Addison-Wesley, Massachusetts, 1956) p. 391.
12. D. C. LUDWIGSON, *Met. Trans.* 2 (1971) 2825.
13. P. MANGANON Jr and G. THOMAS, *ibid.* 1 (1970) 1577.
14. T. H. COLEMAN and D. R. F. WEST, *Met. Tech.* 3 (1976) 49.
15. J. A. VENABLES, *Phil. Mag.* 7 (1962) 35.
16. R. LAGNEBORG, *Acta Met.* 12 (1964) 823.
17. R. E. SHRAMM and R. P. REED, *Met. Trans.* 6A

(1975) 1345.

18. G. B. OLSON and M. COHEN, *ibid.* 6A (1975) 791.
19. D. T. LLEWELLYN and J. D. MURRAY, "Metallurgical Developments in High Alloy Steels", (Iron and

Steel Institute Special Report No. 86, London, 1964) p. 197.

Received 2 May and accepted 30 July 1980.